NanoScience and Technology

Fundamentals of Friction and Wear

von
Enrico Gnecco, Ernst Meyer

1. Auflage

Springer-Verlag Berlin Heidelberg 2006

Verlag C.H. Beck im Internet:
www.beck.de
ISBN 978 3 540 36806 9

Zu Inhaltsverzeichnis

anoscale Friction and Ultrasonics

eresa Cuberes

Mecánica Aplicada e Ingeníera de Proyectos, Universidad de Castilla-La
na, Plaza Manuel de Meca 1, 13400 Almadén, Spain

Introduction

sonic technology finds many applications in our society. It is used in
stry, biology and medicine, i. e. for preparation of colloids or emulsions,
regermination of seeds, for imaging of biological tissues, etc. Also, it is
in nondestructive testing (NDT), for measurement of materials prop-
, in metrology, etc. Ultrasonic vibrations are commonly employed in
anical machining of materials [1]. Procedures such as ultrasonic cut-
of metals, ultrasonically assisted wire-drawing, ultrasonically assisted
g, etc., take advantage of a modification of friction by ultrasonic vibra-
Macroscopically, it is well known that friction and acoustics are very
related [2]. The development of *nanoscale ultrasonics* can be of inter-
nanotechnology. Nevertheless, studies related to the emission of ultra-
from nanoscale contacts or to the influence of ultrasonic vibrations on
friction are still scarce [3].

ne investigation of friction at the nanometer scale can be realized with
omic force microscope (AFM). A specific AFM-mode, friction force mi-
opy (FFM), has been developed for this purpose [4]. FFM monitors
orsion of a microcantilever as a sample is laterally displaced by means
zoelectric actuators, being the cantilever tip in contact with the sam-
rface. Typically, the deformation of the cantilever is sensed by optical
deflection, and both bending in normal direction and torsion are simul-
usly recorded with a four-quadrant photodiode detector [5]. The mea-
ent of the lateral forces that act upon the tip–sample contact during
rd and backward scans allows us to distinguish frictional forces, which
se when reversing the scanning direction, from the lateral forces that
from topographical features. The lateral resolution in FFM depends on
p–sample contact area, which is typically $10-100\,\mathrm{nm}$ in diameter, in
ent conditions.

trasound refers to mechanical vibrations of frequencies ranging from
z up to GHz. Typical ultrasound propagation velocities in solid ma-
s are of the order of $10^3\,\mathrm{m\,s^{-1}}$. Hence, ultrasonic wavelengths in solid
rials are of the order of mm, much larger than the diameter of the mean

ther it is possible to detect ultrasonic vibration at the contact of an AFM
ilever tip and a sample surface is not trivial at first sight. A cantilever
n contact with a surface will certainly be subjected to forces when the
ace atoms displace due to ultrasound excitation, but if the ultrasonic fre-
ncy is sufficiently high, considering the cantilever tip as a point mass,
clear that it will not be able to follow the surface motion due to its
tia.

Starting from 1992, different procedures to monitor ultrasonic vibrations
sample surface using an AFM cantilever tip have been explored, which
be described in this chapter [6–23]. A first motivation for most of those
ies was to implement a near-field approach that provided the kind of
rmation that is obtained with the acoustic microscope, i. e. information
ut the elasticity and viscoelasticity of materials, but with a lateral reso-
on on the nanometer scale. To this aim, different AFM-based techniques
as ultrasonic force microscopy (UFM) [7, 9], atomic force acoustic mi-
copy (AFAM) [10], and heterodyne force microscopy (HFM) [21] have
quite successfully implemented. The different methods and their main
ortunities for the characterization of nanoscale materials properties will
riefly outlined in Sect. 4.2.

Shear ultrasonic vibration excited at a sample surface can also be detected
the tip of an AFM cantilever [24–36]. Experiments that monitor the can-
er response to shear ultrasonic vibration excited at the tip–sample inter-
, with the tip in contact with the sample surface, provide novel methods
tudy nanoscale friction. Some interesting results concerning the response
anocontacts to shear ultrasonic vibration will be introduced in Sect. 4.3.
n Sect. 4.4, experimental evidence of the reduction and/or elimination of
ion at nanometer-sized contacts by means of ultrasonic vibration will be
sidered. The opportunity to control friction at the nanometer scale is of
mendous significance in nanotechnology. By now, it has been unambigu-
y demonstrated that ultrasound of sufficiently high amplitude can act as
oricant in nanoscale contacts [38, 43–45]. Nevertheless, only a few exper-
nts that address this topic have been performed to date, and hence the
ortunities of ultrasonic vibration to modify the mechanisms of friction at
nometer scale are still an open question.

n Sect. 4.5, some attempts to obtain information about adhesion and/or
adhesion hysteresis using ultrasonic AFM techniques will be summa-
d [21, 51–57]. Procedures for the measurement of adhesion hysteresis from
M have been investigated, and a relationship between adhesion hysteresis
friction has been formally established [54]. Phase-HFM provides infor-
ion about dynamic relaxation processes related to adhesion hysteresis
oscale contacts with an extremely high time sensitivity, superior to any
r ultrasonic-AFM procedure [21]. In view of a comparison of phase-HFM
friction data, the opportunities to take advantage of the time resolution

Normal Ultrasonic Vibration at Nanocontacts

e following, we will consider the nanocontact formed by the tip of an cantilever in contact with a sample surface. Normal ultrasonic vibra- at the tip–sample interface can be excited using, for instance, an appro- e piezoelectric element attached to the back of the sample; longitudinal tic waves originated by mechanical vibrations of the piezo will propagate gh the sample, and reach the surface–tip contact area.

s indicated in the introduction, in the limit of high ultrasonic frequen- hundreds of MHz for instance), it is not expected that the cantilever contact with the sample surface can move fast enough to keep up with ce atomic vibrations at ultrasonic frequencies, due to its inertia. Nev- less, the displacement of the surface atoms will lead to modification of p–sample interaction forces. In the absence of ultrasound, with the tip ntact with the sample surface, in the repulsive interaction force regime, antilever is bent to compensate for the sample surface repulsive inter- ns, so that the net force at the tip–sample interface is zero, and the tip ented into the sample to a certain extent, which depends on both the ever and the tip–sample contact stiffness. In the presence of normal ul- nic vibration the tip–sample distance is varied at ultrasonic frequencies en minimum and maximum values, which depend upon the amplitude rasound excitation and the initial set-point force (see Fig. 4.1a). If the tude of the ultrasound is small, the tip–sample distance sweeps a linear of the tip–sample interaction force curve. The net average force that upon the cantilever during an ultrasonic time period will be in this he initial set-point force. However, if the amplitude of ultrasound is ased, and the tip–sample distance is swept over the nonlinear part of orce curve, the average force will then include an additional force. If ltrasonic amplitude is sufficiently high, the cantilever experiences an ional displacement due to this force, which can be easily detected with ptical lever technique [7]. This additional force constitutes the so-called *onic force* and it is the physical parameter evaluated in *ultrasonic force scopy (UFM)* [7,9]. The ultrasonic force induces a static cantilever dis- ment (UFM signal) as long as vertical ultrasonic vibration of sufficiently amplitude is present at the tip–sample contact. In this sense, the can- r behaves as a mechanical diode, and UFM has also received the name chanical-diode ultrasonic mode.

he ultrasonic force is hence understood as the averaged force experi- by the tip during each ultrasonic period. Its magnitude depends upon art of the tip–sample force regime over which the tip–sample distance while being modulated at ultrasonic frequencies, i. e. on the initial ample distance (the initial indentation or set-point force) and on the ul- nic amplitude. The ultrasonic response will be dependent on the details

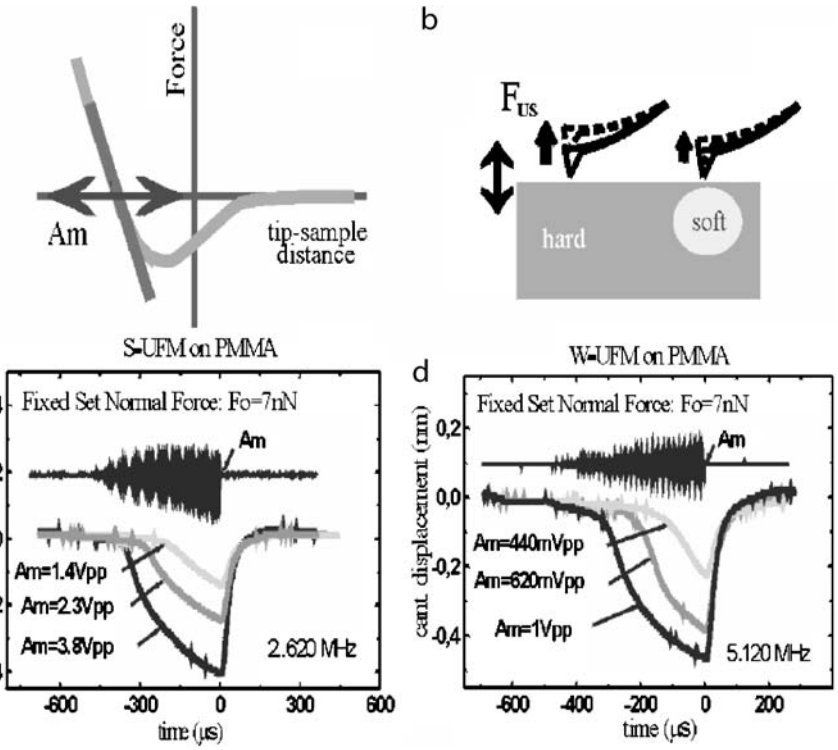

4.1. a,**b** The physical principle of UFM measurements (see text). The ultra- excitation may be introduced through the sample (S-UFM) (**c**) or through ip using the cantilever as a waveguide (W-UFM) (**d**). The piezo excitation is n a triangular modulation, with maximum amplitude A_{m}. The effect of varying static force F_{o} (set-point force) is similar for S-UFM and W-UFM (from [22])

sical principle of the UFM measurements. Softer surface or near-surface ons of nanoscale dimensions at the sample under consideration will be y distinguished from harder regions because of a smaller UFM signal at former (Fig. 4.1b). Fig. 4.1c and d displays UFM responses of a sample of (methylmethacrylate) about 3 mm thick (see [22] for more details about e measurements). As shown in the figure, the piezo excitation is given angular modulation, with maximum amplitude A_{m}. In Fig. 4.1c, the piezo cated at the back of the sample, and works at a frequency of 2.620 MHz way ultrasound is excited at the tip–sample contact in Fig. 4.1d will be ussed below). The set-point force is kept constant at 7 nN. UFM responses different maximum ultrasonic amplitudes are shown. As it is noticeable n the figure, the UFM response is zero until the amplitude of ultrasound tation reaches a threshold value, and it then increases as the ultrasonic

and by monitoring its magnitude at every surface point by means of
-in amplifier, UFM images can be measured. To date, it has already
demonstrated that UFM is a useful technique to map the nanoscale elas-
and adhesive properties of surface and subsurface regions in a variety
h stiff and compliant samples [9, 19].
hen working in the UFM mode, the high-frequency cantilever vibration
directly monitored. If the cantilever is regarded as a simple point mass,
mplitude of vibration at the driving frequency should vanish in the limit
y high frequencies [7]. Nevertheless, the cantilever is not a point mass,
tiny elastic beam that can support high-frequency resonant modes.
ic acoustic force microscopy (AFAM) [10, 13] monitors the resonance
encies of the high-order bending modes of the cantilever, being the tip
e AFM cantilever in contact with the sample surface, in the presence
rmal ultrasonic vibration at the tip–surface interface. According to the
theory of elastic beams, the flexural resonance frequencies of a rectangu-
ntilever are the solutions of a fourth-order differential equation, which
e analytically solved for a clamped-free cantilever, and for a clamped
g-coupled cantilever with the tip in contact with a sample surface [13].
e latter case, the resonances are shifted in frequency and the vibra-
amplitudes along the cantilever changes. Using a linear approximation
e tip–sample interaction forces, the frequency shift can be calculated.
e 4.2 shows the resonance frequencies of the clamped spring-coupled

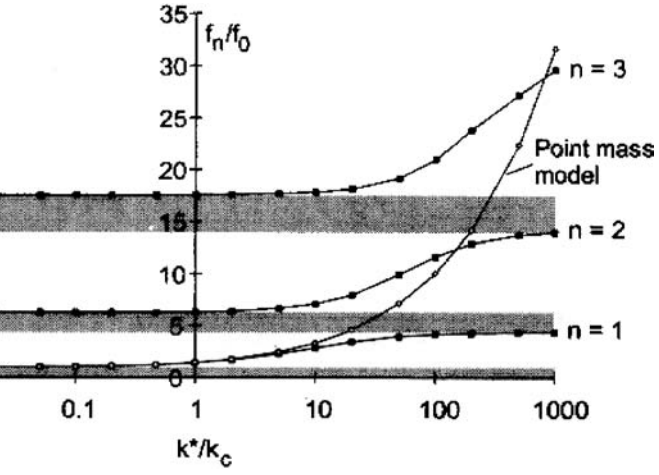

4.2. Resonance frequencies f_n of the clamped spring-coupled cantilever with
p in contact with a sample surface (black squares) normalized to the first
nce frequency of the clamped-free cantilever f_o. K^* and K_c are the tip–
e contact stiffness and the cantilever stiffness, respectively. A comparison

ilever as a function of the stiffness of the tip–sample contact normalized he cantilever stiffness for the first three modes. The experimental deter- ation of the shift of the resonance frequencies of the high-order flexural ilever modes provides a measurement of the tip–sample contact stiffness, lateral resolution in the nanometer scale. From the contact stiffness, the ple indentation modulus can be derived using, for instance, Hertz contact ry [13].

n UFM, it is assumed that the cantilever is *dynamically frozen*, and s not vibrate at ultrasonic frequencies [7]. Even though resonant modes certainly be excited at a microcantilever, the point-mass picture for the M cantilever tip allows us to understand certain peculiarities of its high- uency dynamic behavior. Thus, the inertia of the cantilever "explains" in ultrasonic-AFM techniques soft cantilevers can indent hard samples, yield information about surface and subsurface elastic inhomogeneities. he limit of high ultrasonic frequencies, the amplitude of vibration at the ts of the resonant modes of a clamped spring-coupled cantilever is ex- ed to be very small, and extremely difficult, if possible, to detect. Hence, M appears as the most appropriate technique for measurements at higher asonic frequencies. Typically, in AFAM, the tip–sample distance is kept ciently small that the tip–sample interactions remain in the linear regime. ontrast, UFM relies on the nonlinearity of the tip–sample interaction e; if the tip–sample interactions are in the linear regime, no ultrasonic e is expected to set in at the tip–sample contact.

The detection of surface ultrasonic vibration with the tip of an AFM ilever was first demonstrated in [6] by exciting surface acoustic waves Ws) at slightly different frequencies, and using a cantilever tip in con- with the sample surface to detect the surface vibration at the difference uency. SAWs are acoustic modes that are confined within a wavelength he surface of a solid, and propagate along specific crystalline directions. y can be excited using interdigital transducers (IDTs) on appropriate strates. *Scanning acoustic force microscopy (SAFM)* was particularly im- nented for the characterization of SAW field amplitudes [11] and phase cities [18]. The procedure in SAFM is actually equivalent to this in UFM: superposition of two SAWs of slightly different frequencies leads to surface -frequency vibration that is modulated in amplitude at the (lower) dif- nce frequency. When the surface vibration amplitude is sufficiently high, ntilever tip detects the signal via the mechanical diode effect, due to the linearity of the tip–sample force curve.

n *scanning local acceleration microscopy (SLAM)* [14], the cantilever tip onsidered a point mass. Three different working modes are distinguished: contact-mode, the mechanical-diode mode and the subharmonic mode. In act-mode SLAM, the sample is vibrated at high frequency, with the tip ontact with the sample surface, and the tip displacement, which yields the

ce vibration amplitude is kept sufficiently low that the tip–sample in-
ion remains in the linear regime. The mechanical-diode SLAM mode is
alent to UFM. In subharmonic SLAM, the sample surface is excited at
nigh ultrasonic vibration amplitudes. According to interesting reported
[12], the analysis of the generation of subharmonics and chaos may pro-
nformation about the local coefficient of restitution of a tip bouncing
sample surface.

canning microdeformation microscopy (SMM) [8] uses a piezoelectric ele-
to both excite ultrasonic vibration at a sample, and detect the acoustic
generated by the microdeformations caused by a tip in contact with
mple surface. The technique can operate in transmission mode, with the
located at the back of the sample. In this way, contrast of local elas-
onstants, inhomogeneities and/or subsurface features is obtained with
ral resolution essentially related to the tip diameter.

is worth remarking at this stage that most of the different ultrasonic-
approaches discussed so far have capabilities of *subsurface imaging* [8,
Nevertheless, so far the resolved buried feature sizes are typically much
er than the used acoustic waves, the sensitivity to subsurface features
not appear straightforwardly related to acoustic wave propagation, but
r to a near-field effect.

he development of AFAM has proved that in the presence of ultrasound,
the tip is in contact with a sample surface, flexural resonant modes are
ed at typical AFM cantilevers at frequencies of some MHz. Nevertheless,
usually also works quite well in the frequency range of some MHz. In
mple, the ultrasonic frequency selected for UFM measurements should
e coincident with the cantilever contact resonances in order that the
frequency displacements of the tip are as small as possible. However, it
dditionally been demonstrated that ultrasound can be excited at a sam-
rface from a piezoelement located at the cantilever base. In this case, the
ever acts as an acoustic waveguide that propagates the ultrasonic signal
e sample. As in AFAM, the measurement of the amplitude and resonant
ency of the high-order resonances of a cantilever in contact with the
le surface when ultrasound is excited from the cantilever base provides
mation of the sample elasticity with nanoscale resolution [15, 16]. SMM
lso been implemented in the so-called "reflexion mode", with a piezoele-
located at the cantilever base that is used for both the excitation and
etection of ultrasound [17]. And even though the propagation of ul-
und from the cantilever base to the sample surface necessarily requires
he cantilever tip vibrates at the excitation frequency, it has been exper-
ally demonstrated that UFM works in this configuration, renamed as
guide-UFM (W-UFM) for distinction. As in the case when ultrasound is
ed at the tip–sample contact from the back of the sample (sample-UFM,
M) [22, 23], in W-UFM the ultrasonic excitation is input at the tip–

PMMA can be compared in Fig. 4.1c and d. In Fig. 4.1d, a piezo located he cantilever base is excited at 5.120 MHz. As it is apparent from the re, both procedures lead to remarkably similar qualitative responses. In ciple, excitation of ultrasound from the cantilever base in ultrasonic-AFM niques is potentially advantageous as there are by far fewer restrictions he sample shape or its internal structure (e. g. porous or hollow samples be studied). In addition, the use of same piezo–cantilever–tip assembly different samples simplifies a quantitative comparison of nanoscale me- ical data.

n *heterodyne force microscopy (HFM)* [21], ultrasound is excited both at tip (from a transducer at the cantilever base) and at the sample surface m a transducer at the back of the sample) at adjacent frequencies, and ed at the tip–sample gap (see Fig. 4.3). The physical principle of HFM is ribed in Fig. 4.3. As the sample vibrates at a frequency ω_1 and the tip at equency ω_2, the maximum tip–sample distance, is modulated at $\omega_1 - \omega_2$ t frequency). Provided that the total amplitude is large enough to cover nonlinear range of the tip–sample interaction force, an ultrasonic force onger for larger amplitudes) will act upon the cantilever and displace it

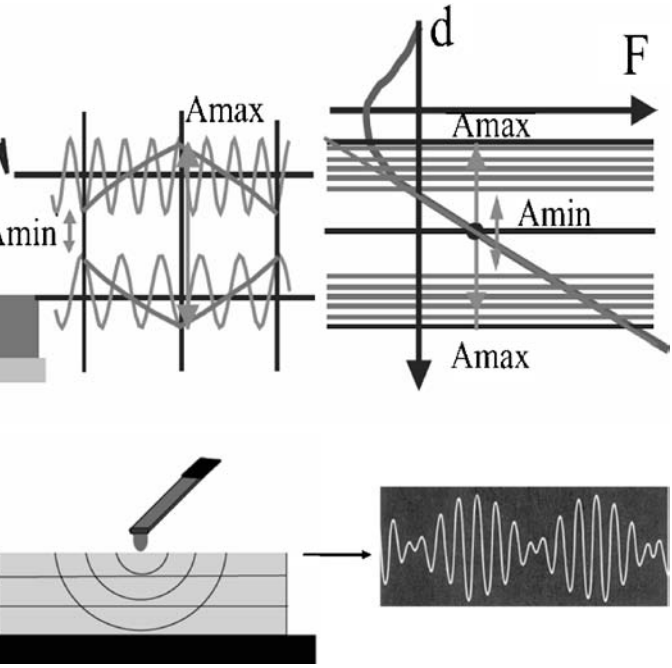

4.3. A schematic diagram illustrating HFM. Small phase delays between tip sample vibration (at ω_1 and ω_2, respectively) will cause a phase variation of

its initial position. Owing to the varying ultrasonic force, the cantilever
tes at the difference mixed frequency. In HFM, this vibration is moni-
in amplitude and phase with a lock-in amplifier, using the (externally)
onically mixed signal as a reference. The information provided by the
tude-HFM (A-HFM) response is very similar to that obtained by UFM.
scale lateral variations in sample elasticity and/or adhesive properties
ive rise to A-HFM contrast. A unique feature of HFM is its ability to
or phase shifts between tip and sample ultrasonic vibrations with an
mely high temporal sensitivity, i. e. fractions of an ultrasonic time pe-
Small differences in the sample dynamic viscoelastic and/or adhesive
nse to the tip interaction result in a shift in phase of the beat signal
s easily monitored in phase-HFM (ph-HFM). In this way, HFM makes
sible to study dynamic relaxation processes in nanometer volumes with
e-sensitivity of nanoseconds.

ecently, *scanning near-field ultrasound holography (SNFUH)* [23] has
proposed as a nondestructive imaging method. The technique is imple-
ed in a similar way to HFM, save that here the difference frequency is
n in the range of hundreds of kHz whereas in [21] difference frequencies of
kHz are used. The experimental data obtained by SNFUH demonstrate
pability to provide elastic information of buried features with great sen-
y. Interestingly, in phase-HFM most of the contrast apparently stems
surface effects, as will be discussed in Sect. 4.5 of this chapter.

Shear Ultrasonic Vibration at Nanocontacts

consider the nanocontact formed by the tip of an AFM cantilever in
ct with a sample surface, shear ultrasonic vibrations at the tip–sample
ace can be excited using, for instance, a shear piezoelectric element
ned to the back of the sample; shear acoustic waves originated by me-
cal vibrations of the piezo will propagate through the sample, and reach
rface–tip contact area.

ith a shear-wave transducer oriented in such a way that the surface in-
vibrations are polarized perpendicular to the long axis of the cantilever,
nal resonant modes of a cantilever with the tip in contact with the sam-
rface are excited. *Lateral-acoustic friction force microscopy (L-AFAM)*
esonant friction force microscopy (R-FFM)) [24–27] monitors the vi-
on amplitudes of the cantilever torsional resonant modes at different
ce points. In this technique, the sample is typically laterally vibrated at
frequencies, and the torsional vibration amplitudes provide information
the lateral forces between tip and sample. Apparently, L-AFAM images
dependent of the scanning direction, i. e. not influenced by topography-
ed lateral forces [25]. When scanning in the presence of shear ultrasonic

$-250\,\mu\mathrm{ms}^{-1}$), and nearer to the sliding operating velocities in MEMs and Ms (in the range of tens of $\mathrm{mm\,s}^{-1}$ to a few ms^{-1}) [37].

The analysis of the torsional contact resonances of AFM cantilevers in act with a sample surface provides a novel means to study friction and k–slip phenomena at the nanometer scale [26,27]. At low shear-excitation ages, the resonance curve torsional cantilever vibration amplitude versus tation frequency is a Lorentzian with a well-defined maximum; the can- er with the AFM tip stuck to the sample surface following the surface ion, behaves like a linear oscillator with viscous damping. Above a critical r excitation amplitude, which depends on the static cantilever load, and the order of 0.2 nm for bare and lubricated silicon samples [26], the shape he resonance curve exhibits a characteristic flattening, attributable to the et of sliding friction at the tip–sample contact. Experimental evidence of gy dissipation before sliding friction sets in has been related to microslip, slipping of an annulus at the tip–sample contact before the whole contact ts to slide (see Ref. [26] for further details).

The local vibration amplitudes and phases of the torsional resonances of nped-free AFM cantilevers have been studied using optical interferome- [28]. The finite size of the cantilever beam and asymmetries in its shape s to coupling between flexural and torsional vibrations. Lateral resonant es of AFM cantilevers, which consist in flexural vibration modes in the ilever width direction parallel to the sample surface, have also been ex- mentally observed [29]; asymmetries in the cantilever thickness lead to component of the displacement that can be monitored by optical beam ection with an AFM.

The torsional resonant modes of a cantilever tip in contact with a sample ace have also been excited using a shear piezo located at the cantilever e [30,31]. In the *torsional resonance dynamic-AFM mode (TR mode)* [32] ional vibrations of the cantilever are excited via two piezoelectric elements nted beneath the holder of the chip, which vibrate out-of-phase, in such y that they generate a rotation at the length axis of the cantilever. Using procedure, the torsional resonances of the cantilever can be monitored in n near-contact and contact modes. In ultrahigh vacuum (UHV), torsional ilever resonances can be excited via vertical vibrations, due to their high ity factors. Lateral forces between a cantilever tip and objects on sur- s have been measured in UHV by monitoring the induced change of the uency of the fundamental cantilever torsional resonant mode [33]. In the *ional overtone microscopy* [34], torsional cantilever resonances excited hermal noise are used to obtain information about the shear stiffness of tip–sample contact.

In the limit of high ultrasonic frequencies, it is questionable if high-order ional resonances will be excited at the cantilever. Nevertheless, in *lateral ning acoustic force microscopy (LFM-SAFM)* [35,36] SAWs with inplane

ample surface, in the presence of shear ultrasonic vibration at the tip–
e contact, the cantilever experiences an additional amplitude-dependent
n or lateral mechanical-diode effect. From the ultrasound-induced addi-
torsion, information about the amplitude and phase velocity of in-plane
ized SAWs can be obtained.
lateral ultrasonic force microscopy (L-UFM) [9] lateral vibrations of the
e surface at a relatively low frequency of some kHz, polarized perpen-
r to the length axis of the cantilever, are superimposed on a continuous
al ultrasonic surface vibration. The measurement of the amplitude of
n of the cantilever at the lateral low-frequency surface vibration pro-
information about the sample shear elastic properties with subsurface
ivity.

Reduction of Friction by Ultrasonic Vibration

eduction of friction by ultrasound is a well-known macroscopic effect [1,
occurrence at the nanometer scale is only recently being investigated.
inelli et al. [38] studied the influence of out-of-plane ultrasonic vibration
e frictional response of a Si sample in ambient conditions, using FFM
UFM. Their results clearly demonstrated that dynamic friction vanishes
presence of ultrasound when the tip–surface contact breaks for part of
ut-of-plane vibration cycle (see Fig. 4.4). Figure 4.4 shows the friction
and the cantilever deflection measured at different surface ultrasonic
tion amplitudes. The friction force in Fig. 4.4 was independently deter-

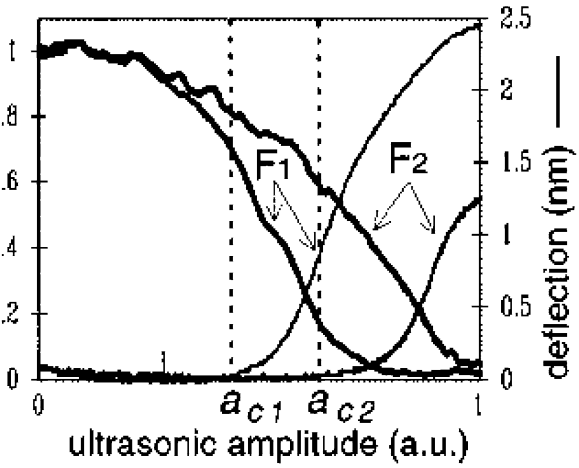

4.4. Experimental measurements of dynamic friction (thick line) and can-

ed for each of the different amplitudes of surface ultrasonic vibrations by
rally scanning the sample back and forth in the direction perpendicular
he cantilever axis, using a lock-in amplifier (see Ref. [38] for further de-
). The cantilever deflection signal in Fig. 4.4 corresponds to the cantilever
onse to the ultrasonic force, i. e. the UFM signal, which depends on the
asonic amplitude (see Fig. 4.1). The onset of an UFM response for a given
oint force roughly indicates the ultrasonic amplitude needed for the tip
etach from the sample surface at part of the surface ultrasonic vibration
e.

The breaking of the tip–sample contact at each ultrasonic cycle explains
reduction or elimination of friction because of a reduction of slippage
ng sliding. Interestingly, it is apparent from Fig. 4.4 that, for a given
ied load, the friction force considerably decreases well before the onset
he UFM response, i. e. while the tip remains in "linear contact" with the
ple surface during the ultrasonic vibration cycle. For the case of F_2 in
4.4, the reduction of friction already amounts to about 60% when the
M cantilever response sets off.

The influence of normal ultrasonic vibration on the static friction force was
ied by keeping the amplitude of the lateral displacement small enough
the tip remained stick to a surface point without sliding, see Ref. [38] for
ils. It was demonstrated that the static friction force begins to decrease at
low ultrasonic amplitudes, and that the onset of friction reduction does
depend on the applied shear force. Evidence on this latter point ruled
the possibility that the reduction of friction is due to slippage during the
of the period that the tip–sample forces are the lowest.

In order to explain a reduction of friction at low ultrasonic amplitudes,
presence of a surface layer at the tip–sample gap, i. e. a liquid layer formed
vater and possibly organic contaminants, has been considered [38]. In the
ence of ultrasonic vibration, such a layer might organize in a solid-like
figuration between the tip and the sample and partially sustain the load.
he tip–sample distance is varied at ultrasonic frequencies, the viscosity
he layer would hinder its rearrangement, thereby reducing the probability
p stick–slip processes, and hence friction.

Using molecular dynamics (MD) simulations, Gao *et al.* [39] demonstrated
small amplitude (of the order of 0.1 nm) oscillatory motion of two con-
g interfaces in the normal direction to the shear plane can lead to tran-
ns of a lubricant from a high-friction stick-slip shear dynamics to an
alow kinetic friction state (superkinetic friction regime), provided that
characteristic relaxation time for molecular flow and ordering processes
he confined region is larger than the time constant of the out-of-plane
hanical oscillations.

Heuberger et al. [40] observed load- and frequency-dependent transitions
ween a number of dynamic friction states of a lubricant using a surface

ing normal vibrations between two boundary-lubricated sliding surfaces. rticular, they found regimes of vanishingly small friction at interfacial os- on amplitudes below 0.1 nm, and demonstrated that they originate due e dynamics of the relaxation processes of the lubricant at the molecular

ecently, Socoliuc et al. [41] have demonstrated that mechanical vibra- normal to the plane of sliding at cantilever resonance frequencies in the of hundreds of kHz in ultrahigh-vacuum (UHV) conditions lead to an ow friction regime in atomic scale friction even when the amplitude is fficiently high that the tip detaches from the sample during the vibra- ycle. Previously [42], the authors had reported on the observation of an ow dissipation state in atomic friction related to the absence of mechan- stabilities, attained by varying the normal force. Such a state may exist se a modification of the tip–sample normal load leads to changes in the l surface corrugation felt by the tip without significantly altering the ess of the tip–sample contact. In the case that the tip–sample force is dically varied at high frequencies, it is feasible that the tip slides through ow dissipation atomic friction states when being laterally displaced.

he effect of in-plane ultrasonic vibration in nanoscale friction has also considered. Scherer et al. [25] observed that when lateral ultrasonic vi- ons are excited at a sample surface at ambient conditions using a shear bonded to the back of the sample, friction nearly vanishes at certain ency bands, whereas it remains as high as on a nonvibrating surface at frequencies. However, they verified that the near-zero friction bands co- d with frequencies at which a lift-off (vertical displacement) of the AFM ever occurred. As discussed by the authors [25] such "lift-off" might be uted to the set in of a vertical ultrasonic force due to parasitic out-of- motions of the sample surface or to mode coupling in the cantilever. theless, the buildup of an elastohydrodynamic lubrication film whose sity and hence thickness is dependent on the lateral tip–sample relative ty was proposed as a reasonable hypothesis that could account for a ver- cantilever displacement in the absence or in the case of low-amplitude f-plane surface vibrations.

ehme et al. [43–45] studied the influence of surface acoustic waves Vs) on nanoscale friction. SAWs constitute a precise source of acous- oration, with well-defined surface oscillations in a perfectly determined ization, whereas when working with bulk shear-wave transducers para- urface displacements due to the existence of boundaries, etc. can hardly oided. LFM and multimode SAFM were used to measure and distin- the influence of inplane and vertical surface oscillations components on antilever torsion and bending. To this aim, the authors [43–45] excited nding Rayleigh-wave field, and considered the dependence of friction e acoustic excitation amplitude. In Rayleigh waves, the atoms oscil-

tion component. The experiments showed that by increasing the rf amude, friction is locally reduced an eventually suppressed. In addition, it clearly demonstrated that at the point at which friction disappears, the ral-SAFM signal breaks down. Hence, it was concluded that the effect iction reduction is essentially due to the vertical mechanical-diode effect leads to an effective shift of the cantilever, whereas inplane oscillations ot play a significant role. This hypothesis was further reinforced by the that apparently in-plane polarized Love-type SAWs did not significantly the frictional behavior. When using the in-plane polarized Love-type Vs, no cantilever lift-off induced by a lateral oscillation of the sample was erved [25]. At very high Rayleigh-wave amplitudes a lateral force rectifica- of the longitudinal component of the standing-wave field was apparent, ch resulted in a scan-direction-independent appearance of the LFM traces. Ultrasonic vibration covers a broad range of frequencies, and the processes lved in a reduction of friction by ultrasound can vary at different relative sample velocities. De Hosson and Kessermakers [46] studied the influence anoscale friction of lateral high-frequency vibration of the cantilever, o frequencies of 1 MHz, on a NbS_2 sample at ambient conditions, and erved gaps of lowered or eliminated friction at specific frequencies, pred to be around torsional and/or lateral cantilever resonances. In these eriments a Au-coated cantilever was used, and the oscillating lateral canver vibration was applied by means of an electrostatic field. At a particfriction-gap frequency, a slow increase in driving field amplitude caused adual increase in friction, and above a certain threshold level of driving olitude, a partial stick-slip behaviour with the tip periodically alternating ween a zero friction an a nonzero-friction state was apparent.

Riedo et al. [47] also reported about a reduction of friction when lateral llations around a frequency of 19.5 kHz were applied to an AFM cantilever ng on mica. In the range of scanning velocities they used, the thermally vated hopping of contact atoms over the effective lateral interatomic poial led to increased energy dissipation when increasing the sliding velocity. superimposing a lateral oscillation on the cantilever and sweeping its frncy between about 20 to 300 kHz, and a clear peak of friction-reduction observed around 19.5 kHz, independently of the applied load. This fricreduction peak was attributed to the excitation of a cantilever torsional act resonance, which increased the attempt frequency for thermally acti- jumps during sliding. The effect did not occur above a certain critical e of the sliding velocity.

In recent experiments performed by Socoliuc et al. [41] on KBr samples UHV no reduction-of-friction effect was apparent upon the excitation of ional cantilever contact resonances in the frequency range from 40 kHz up 00 kHz, even though friction was strongly reduced when the excitation uency matched one of the normal resonance frequencies of the pinned

ther studies that have considered the possibility to control nanoscale on by mechanical action at high frequencies on the system motion are bed in [48, 49] and Ref. therein.

Adhesion Hysteresis at Ultrasonic Frequencies

ne nanoscale, adhesion phenomena become decisive to the performance nodevices, and surface properties acquire a particular relevance. Usually, ork of adhesion is defined as the energy needed to separate two surfaces, ming that this is reversible [50]. The adhesion hysteresis is defined as the ence between the work needed to separate two surfaces and that gained bringing them together. The fact that those two works are different agnitude, i. e. the adhesion hysteresis is different from zero, can be at-ed to elastic, viscoelastic and plastic deformations in the contact zone, figuration of surface molecules during contact, chemical reactions, etc. ecently, novel methods to obtain information about the work of adhe-and the adhesion hysteresis at the tip–sample contact using UFM have proposed [51–55]. Essentially, they take advantage of the fact that the sonic amplitude at which an UFM response sets off when increasing xcitation is different from this at which it falls down when decreasing xcitation. This is illustrated in Fig. 4.5 [51], in which both experimen-d simulated UFM signal versus ultrasonic excitation amplitude curves been drawn. In UFM, with the tip in contact with the sample, when

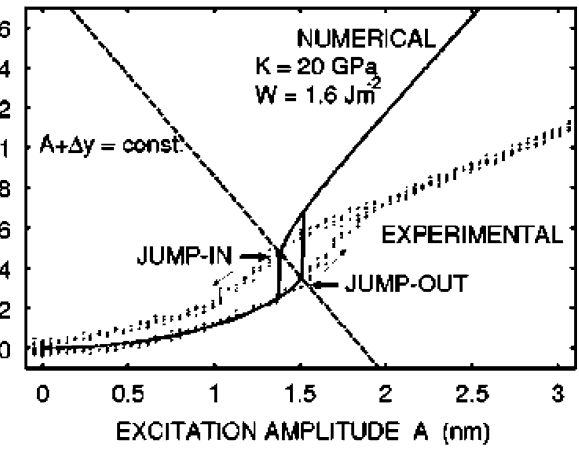

4.5. UFM signals recorded when increasing and decreasing the ultrasonic tion amplitude (see arrows to distinguish each case) on an aluminum thin film. ontinuous lines correspond to a numerical evaluation of the UFM responses

easing the normal ultrasonic amplitude at the tip–sample contact, at ain amplitude the tip detaches from the surface at part of the ultra- c period, and the ultrasonic force (see Sect. 4.2 of this chapter) experi- s a sudden increase that gives rise to a "jump-out" of the cantilever (see 4.5). When decreasing the ultrasonic amplitude, at certain amplitude tip can no longer separate from the surface, and the ultrasonic force ex- ences a sudden decrease that gives rise to a "jump-in" of the cantilever Fig. 4.5). For the evaluation of the ultrasonic force, it is considered that hanical hystereses, i. e. snap-in and -out of the cantilever when approach- or separating from the sample surface do not occur. In the absence of asound, compliant cantilevers are subjected to large mechanical hystere- when approaching or separating from a sample surface due to the force lient being larger than the cantilever spring constant. However, at ultra- c frequencies, the inertia of the cantilever leads to an effectively much er cantilever stiffness, and the cantilever can probe the hysteretic cycle p–sample in-and-out interactions without a decrease of its sensitivity for e-field detection.

n [51] a method for quantitative analysis of the UFM signal is proposed rder to determine both the sample elastic modulus and the work of adhe- by monitoring the cantilever jumps such as those in Fig. 4.5. In UFM, n elasticity and adhesion contribute to the ultrasonic force. Dinelli et 56] evaluated the contact stiffness by comparing the jump-in positions in asonic amplitude for different applied loads. Using the Johnson–Kendall– erts–Sperling (JKRS) model to account for both elastic and adhesive es between tip and sample, the authors in [51] evaluated both the stiff- and the work of adhesion as defined in JKRS by calculating the jump-in jump-out cantilever shifts. According to their modeling, the normalized ilever jump-in shift turns out to be constant and effectively independent he set-point force, the stiffness and the work of adhesion. Hence, they ved a universal relation between the work of adhesion, the stiffness and cantilever shift at jump-in, the latter being easily measured from the erimental data (see Ref. [51] for further details).

n [52] the area between experimental curves such as those in Fig. 4.5 neasured and defined as the UFM hysteresis area (UH), and it is as- ed that UH scales with the local adhesion hysteresis. A detail procedure btain quantitative information about the adhesion hysteresis from UFM al versus ultrasonic excitation amplitude curves is discussed in [55]. The elations between adhesion hysteresis and local friction have been theo- cally and experimentally investigated [54]. According to a model based he classical theory of adhesional friction and contact mechanics, which udes the effects of capillary hysteresis and nanoscale roughness and as- es an adhesive, elastic and wearless tip–sample contact, a relationship ween adhesion hysteresis and friction has been derived, which depends

g's modulus (see Ref. [54] for further details). In the model, the ad-
n hysteresis is estimated as the pull-off force times the critical separa-
at which the tip–sample contact is about to be broken. Measurements
wide range of engineering samples with varying adhesive and elastic
rties have confirmed the model [52, 54]. The aforementioned ratio does
ary much between typical metallic samples, and for a limited number
ecimen's adhesion hysteresis and friction the experimental relationship
appear linear. In addition, it is found that capillary hysteresis offsets
easured adhesion hysteresis from the friction force, and that roughness
es both friction and adhesion hysteresis: friction decreases because of
ller area of a real contact, and adhesion hysteresis drops due to a smaller
ff force at rough surfaces. Recently, it has been demonstrated that the
of the dependence of local adhesion hysteresis on relative humidity
UFM may provide information about protein–water binding capacity
molecular-scale resolution [53].
rocedures to obtain information about the work of adhesion using AFAM
so being considered [54]. In AFAM, the tip–sample contact stiffness can
termined by monitoring the resonance frequency of an AFM cantilever
contact with the sample surface (see Sect. 4.2 of this chapter). Strictly,
ontact stiffness is influenced by both the tip–sample elastic properties
he work of adhesion. Typically, the tip–sample distance in AFAM is kept
iently small that the tip–sample interactions remain in the linear regime.
ntly, a method has been proposed to evaluate both these properties
itatively from the analysis of the nonlinear AFAM cantilever response
d when the tip–sample distance sweeps the nonlinear part of the tip–
e interaction in such a way that the tip always remains in contact with
mple surface, considering the case of a perfect contact. To this aim, the
dence of the resonance frequency on the vibration amplitude is studied;
astic properties and the work of adhesion are separately determined by
g the optimal set of values that minimizes the difference between the
etical and empirical relationship of cantilever resonance frequency versus
sonic excitation amplitude (see Ref. [56] for further details).
HFM, the phase signal provides information of the adhesion hysteresis
d to the formation and breaking of the tip–surface contact [21]. Contrast
ase-HFM mostly stems from dissipative processes. An exceptional fea-
f this technique is its ability to probe a local response in extremely short
HFM may test effects that take place at nanoseconds in nanometer-scale
nes. Hence, phase-HFM can reveal dissipation due to extremely quick
tions that otherwise remains unresolved from other dissipative effects
ring at larger time scales. For instance, using phase-HFM, it has been
le to distinguish differences in contrast at identical thin polymer layers
different boundary constraints on the nanometer scale. These layers,
ver, exhibited the same FFM contrast, which confirms the ability of

e than conventional FFM. In the following, the results presented in [21] tive to those experiments will be summarized here, with a main focus in erstanding the opportunities of phase-HFM to provide information about esion hysteresis with extremely high time sensitivity.

In metals, anelastic or viscoelastic contributions are expected to be small. ontrast, in polymeric materials, intra- or intermolecular perturbations in- ed by tip actuation, and/or dissipative effects of the molecules due to ad- on to the tip or to other neighboring molecules will play a significant role he phase-HFM contrast. Phase-HFM has been applied to PMMA/rubber ocomposites that consist in an acrylic matrix, a copolymer based upon MA and toughening particles composed of a core of acrylic enclosed with ber with a bonded acrylic outer shell to ensure good bonding to the matrix Fig. 4.6).

Figure 4.6a–c shows contact-mode AFM (a), phase-AFM (b) and LFM ges recorded over the same surface region of a PMMA/rubber sample. topographic protrusions in Fig. 4.6a indicate the presence of core-shell MA particles in the surface and/or near surface region. Two different s of topographic protrusions may be distinguished from those and other ges recorded on the PMMA/rubber sample surface: (i) some that give to a lower Ph-HFM contrast than the PMMA matrix, and (ii) others show a Ph-HFM contrast similar to that of the PMMA matrix. Such

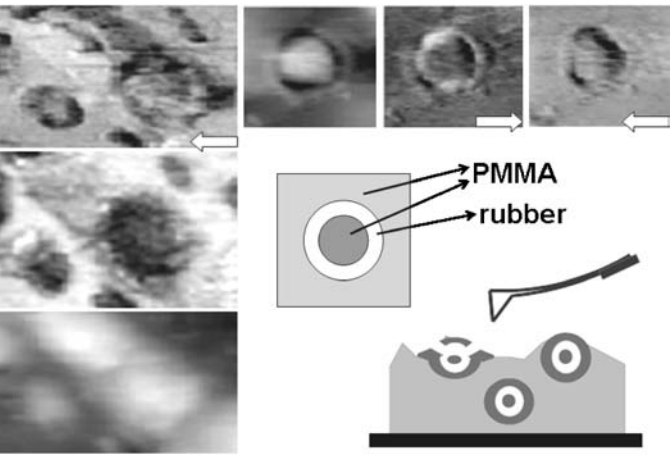

4.6. a–c AFM contact-mode topography (**a**), Phase-AFM (**b**) and LFM (**c**) ges recorded over a same surface region of a PMMA/rubber sample. The images he top right-hand side correspond to AFM contact-mode topography, and LFM ges recorded scanning from left to right, and vice versa respectively (see arrows), a same surface region of the sample, different from that in (**a–c**). Below, matic drawings illustrate the apparent structure at the PMMA/rubber sample

ent protrusions are apparent from the comparison of Fig. 4.6a and b. drawings in Fig. 4.6 illustrate a model for the two different protrusions: me particles, the PMMA particle shell is well-bonded and indistinguish- from the PMMA matrix, whereas in others the rubber particle is still ed with the PMMA layer, but this is detached from the matrix material. a picture is corroborated when considering FFM images (see Fig. 4.6c) ll as UFM and A-HFM images recorded in the same surface region (not n here, see Ref. [21]). Both UFM and A-HFM reveal the presence of oughening particles by a darker contrast, indicative of the presence of er material in the surface or near-surface region. The aforementioned ent particles cannot be distinguished from the UFM and A-HFM mea- nents [21]. However, they are clearly differentiated in Ph-HFM, and dis- ble by the presence or absence of a kind of halo contrast in FFM.

t the top right-hand side of Fig. 4.6, contact-mode AFM and FFM im- recorded over a particular PMMA/rubber particle scanning from left ght (forward scan), and vice versa (backward scan, see arrows in the) are shown. This particle is representative of those that typically give o Ph-HFM contrast, and the image quality is a little better than this g. 4.6c. From those images it is apparent that the particle is character- by a halo-shaped frictional contrast, in both forward (bright halo) and sed (dark halo) FFM scans, which can be attributed to the presence ober directly exposed at the sample surface. Notice that *the PMMA on top of the rubber exhibits the same frictional contrast as the PMMA x, being indistinguishable from that in both forward and backward FFM* . In contrast, Ph-HFM resolves small differences in viscoelastic and/or ion hysteresis response time of the PMMA on top of the rubber that is nked to the PMMA rubber matrix. Relaxation processes of polymeric rials are strongly dependent on the constraints for molecular movement. ferent molecular density, entanglement density and/or molecular weight e PMMA layer on top of the rubber that is detached from the PMMA x may lead to differences in the PMMA viscoelastic and/or adhesion resis response. In addition differences in interfacial bonding between the er and the PMMA on top depending on whether the PMMA is well ad- to the PMMA matrix or not, may also modify the PMMA dynamic vior. According to the obtained experimental results, the contrast pro- by Ph-HFM allows us to distinguish differences in the locally probed mical response of PMMA on top of rubber depending on whether the MA is well adhered to the matrix or not, in spite of the fact that no ence can be resolved in conventional FFM. Hence, Ph-HFM allows us udy quick dissipative transitions not resolved by FFM that, however, play an important role in MEM/NEMs devices working at much higher g velocities than those typically used in AFM/FFM measurements.

is also worth noting that, when probed with extreme sensitivity, a lo-

s induced by long-range interactions (via molecular entanglements) at ecules outside the immediate contact region. The possibility that those ls of interactions might be detected in an extremely short time scale can of interest in the implementation of dynamic mechanical procedures for munications in nanodevices.

nowledgement. E. Gnecco is gratefully acknowledged for scientific discussions, careful reading of the manuscript. Financial support from the Spanish Minis- de Educación y Ciencia (MEC) under project MAT2002-00076), the Junta de unidades de Castilla-La Mancha (JCCM) under projects PBI-02-003 and PBI-18, and the European Science Foundation (ESRF), under the ESRF Scientific gramme NATRIBO, is also gratefully acknowledged.

ferences

See, e. g. *Review on ultrasonic machining*. T.B. Thoe, D.K. Aspinwall, and M.L.H. Wise, Int. J. Mach. Tools Manufact. 38 (1998) 239 and Ref. therein.

See, e. g. *Acoustics of friction* A. Akay, J. Acoust. Soc. Am. 111 (2002) 1525 and Ref. therein.

See, e. g. K. Dransfeld, *Generation of ultrasonic waves in sliding friction*, Chap. 7 in *Nanoscience: Friction and Rheology on the Nanometer Scale*, ed. E. Meyer, R.M. Overney, K. Dransfeld, and T. Gyalong, World Scientific (1998) and refs. therein; this chapter and refs. therein.

Atomic scale friction of a tungsten tip on a graphite surface, C.M. Mate, G.M. McClelland, R. Erlandsson, and S. Chiang, Phys. Rev. Lett. 59 (1987) 942.

Simultaneous measurement of lateral and normal forces with an optical-beam-deflection atomic force microscope, G. Meyer and N. Amer, Appl. Phys. Lett. 57 (1990) 2089.

Detection of Surface Acoustic Waves by Scanning Force Microscopy, W. Rohrbeck and E. Chilla, Phys. Stat. Sol. (a) 131 (1992) 69.

Nonlinear detection of ultrasonic vibrations in an Atomic Force Microscope, O. Kolosov and K. Yamanaka Jpn. J. Appl. Phys. 32 (1993) L1095.

Scanning microdeformation microscopy, B. Cretin and F. Sthal, Appl. Phys. Lett. 62 (1993) 829.

Ultrasonic Force Microscopy for nanometer resolution subsurface imaging, K. Yamanaka, H. Ogiso, and O. Kolosov, Appl. Phys. Lett. 64 (1994) 178.

Acoustic Microscopy by Atomic Force Microscopy, U. Rabe and W. Arnold, Appl. Phys. Lett. 64 (1994) 1493.

Scanning acoustic force microscopy measurements in grating-like electrodes, T. Hesjedal, E. Chilla and H.-J. Froehlich, Appl. Phys. A 61 (1995) 237.

Nanosubharmonics: the dynamics of small nonlinear contacts, N.A. Burnham, A.J. Kulik, G. Gremaud, and G.A.D. Briggs, Phys. Rev. Lett. 74 (1995) 5092.

Vibrations of free and surface-coupled atomic force microscope cantilevers: the-

canning local-acceleration microscopy, N.A. Burnham, A.J. Kulik, G. Gre-aud, P.J. Gallo, and F. Oulevey, J. Vac. Sci. Technol. B 14 (1996) 794.
ltrasonic Atomic Force Microscopy with overtone excitation of the cantilever, . Yamanaka and S. Nakano, Jpn. J. Appl. Phys. 35 (1996) 3787.
ontact imaging in the AFM using a high order flexural mode combined with new sensor, S.C. Minne, S.R. Manalis, A. Atalar and C.F. Quate, Appl. Phys. ett. 68 (1996) 1427.
canning microdeformation microscopy in reflexion mode, P. Variac and . Cretin, Appl. Phys. Lett. 68 (1996) 461.
anoscale determination of phase velocity by scanning acoustic force mi-roscopy, E. Chilla, T. Hesjedal, and H.-J. Fröhlich, Phys. Rev. B 55 (1997) 5852.
lapping surface elastic properties of stiff and compliant materials on e nanoscale using ultrasonic force microscopy, F. Dinelli, M.R. Castell, .A. Ritchie, N.J. Mason, G.A.D. Briggs, and O.V. Kolosov, Philos. Mag. A (2000) 2299.
Vaveguide ultrasonic force microscopy at 60 MHz, K. Inagaki, O. Kolosov, . Briggs, and O. Wright, Appl. Phys. Lett. 76 (2000) 1836.
eterodyne force microscopy of PMMA/rubber nanocomposites: nanomapping f viscoelastic response at ultrasonic frequencies, M.T. Cuberes, H.E. Assender, .A.D. Briggs, and O.V. Kolosov, J. Phys. D.: Appl. Phys. 33 (2000) 2347.
onlinear detection of ultrasonic vibration of AFM cantilevers in and out of ontact with the sample, M.T. Cuberes, G.A.D. Briggs, and O. Kolosov, Nan-echnology 12 (2001) 53.
anoscale imaging of buried structures via Scanning Near-Field Ultrasound olography, G.S. Shekhawat and V.P. Dravid, Science 310 (2005) 89.
ocal Elasticity and Lubrication Measurements Using Atomic Force and Fric-on Force Microscopy at Ultrasonic Frequencies, V. Scherer, B. Bhushan, . Rabe, and W. Arnold, IEEE Trans. Magn. 33 (1997) 4077.
ateral Force Microscopy Using Acoustic Force Microscopy, V. Scherer, . Arnold, and B. Bhushan, Surf. Interface Anal. 27 (1999) 578.
n the nanoscale measurement of friction using atomic-force microscopy can-ever torsional resonances, M. Reinstädtler, U. Rabe, V. Scherer, U. Hartnann, . Goldade, B. Bhushan and W. Arnold, Appl. Phys. Lett. 82 (2003) 2604.
nvestigating ultra-thin lubricant layers using resonant friction force mi-roscopy, M. Reinstädtler, U. Rabe, A. Goldade, B. Bhushan and W. Arnold, ribol. Int. 38 (2005) 533.
naging of flexural and torsional resonance modes of atomic force microscopy antilevers using optical interferometry, M. Reinstädtler, U. Rabe, V. Scherer, .A. Turner, and W. Arnold, Surf. Sci. 532 (2003) 1152.
naging using lateral bending modes of atomic force microscopy cantilevers, . Caron, U. Rabe, M. Reinstätler, J.A. Turner, and W. Arnold, Appl. Phys. ett. 85.
uantitative elasticity evaluation by contact resonance in an atomic force mi-roscope, K. Yamanaka and S. Nakano, Appl. Phys. A 66 (1998) S313.
lapping of lateral vibration of the tip in atomic force microscopy at the rsional resonance of the cantilever, T. Kawagishi, A. Kato, U. Hoshi,

Imaging and measurement of elasticity and friction using the TRmode, M. Reinstädtler, T. Kasai, U. Rabe, B. Bhushan, and W. Arnold, J. Phys. D: Appl. Phys. 38 (2005) R269.
Lateral-force measurements in dynamic force microscopy, O. Pfeiffer, R. Bennewitz, A. Baratoff, E. Meyer and P. Grütter, Phys. Rev. B 65 (2002) 161403.
Determination of shear stiffness based on thermal noise analysis in atomic force microscopy: passive overtone microscopy, T. Drobek, R.W. Stark, and W.M. Heck, Phys. Rev B 64 (2001) 0454001.
Transverse surface acoustic wave detection by scanning acoustic force microscopy, G. Bheme, T. Hesjedal, E. Chilla, and H.-J. Fröhlich, Appl. Phys. Lett. 73 (1998) 882.
Simultaneous bimodal surface acoustic-wave velocity measurements by scanning acoustic force microscopy, G. Behme and T. Hesjedal, Appl. Phys. Lett. 77 (2000) 759.
Recently, a novel AFM-based technique for studying nanoscale friction at velocities near to 10 nm s^{-1} has been implemented; see *A new atomic force microscopy based technique for studying nanoscale friction at high sliding velocities*, N.S. Tambe and B. Bhushan, J. Phys. D: Appl. Phys. 38 (2005) 764.
Ultrasound induced lubricity in microscopic contact, F. Dinelli, S.K. Biswas, G.A.D. Briggs, and O.V. Kolosov, Appl. Phys. Lett. 71 (1997) 1177.
Friction control in thin-film lubrication, J. Gao, W.D. Luedtke, and U. Landman, J. Phys. Chem. B 102 (1998) 5033.
Coupling of normal and transverse motions during frictional sliding, M. Heuberger, C. Drummond, and J. Israelachvili, J. Phys. Chem. B 102 (1998) 5038.
A. Socoliuc, E. Gnecco et al., submitted.
Transition from stick-slip to continuous sliding in atomic friction: entering a new regime of ultralow friction, A. Socoliuc, R. Bennewitz, E. Gnecco, and E. Meyer, Phys. Rev. Lett. 92.134301 (2004).
Influence of ultrasonic surface acoustic waves on local friction studied by lateral force microscopy, G. Behme and T. Hesjedal, Appl. Phys. A 70 (2000) 361.
Influence of surface acoustic waves on lateral forces in scanning force microscopies, G. Behme and T. Hesjedal, J. Appl. Phys. 89 (2001) 4850.
The origin of ultrasound-induced friction reduction in microscopic mechanical contacts, T. Hesjedal and G. Behme, IEEE Trans. Ultrason. Ferroelec. Freq. Cont. 49 (2002) 356.
Probing the interface potential in stick/slip friction by a lateral force modulation technique, J. Kerssemakers and J.T.M. De Hosson, Surf. Sci. 417 (1998) 281.
Interaction potential and hopping dynamics governing sliding friction, E. Riedo, E. Gnecco, R. Bennewitz, E. Meyer, and H. Brune, Phys. Rev. Lett. 91 (2003) 084502-1.
The nonlinear nature of friction, M. Urbakh, J. Klafter, D. Gourdon, and J. Israelachvili, Nature 430 (2004) 523 and Ref. therein.
Tuning diffusion and friction in microscopic contacts by mechanical excitations, Z. Tshiprut, A.E. Filippov, and M. Urbakh, Phys. Rev. Lett. 95 (2005) 0166101.
Chapter 15 in *Intermolecular and surface forces*, J. Israelachvili, Academic Press, Elsevier Ltd., 2nd edn (1992).
Hysteresis of the cantilever shift in ultrasonic force microscopy, K. Inagaki,

ribology and ultrasonic hysteresis at local scales, R. Szoszkiewicz, B.D. Huey, .V. Kolosov, G.A.D. Briggs, G. Gremaud, A.J. Kulik, Appl. Surf. Sci. 219 2003) 54.

robing local water contents of in vitro protein films by ultrasonic force mi-roscopy, R. Szoszkiewicz, A.J. Kulik, G. Gremaud and M. Lekka, Appl. Phys. ett. 86 (2005) 123901.

orrelations between adhesion hysteresis and friction at molecular scales, . Szoszkiewicz, B. Bhushan, B.D. Huey, A.J. Kulik, and G. Gremaud, J. Chem. hys. 122 (2005) 144708.

uantitative measure of nanoscale adhesion hysteresis by ultrasonic force mi-roscopy, R. Szoszkiewicz, A.J. Kulik, and G. Gremaud, J. Chem. Phys. 122 2005) 134706.

leasurements of stiff-material compliance on the nanoscale using ultrasonic rce microscopy, F. Dinelli, S.K. Biswas, G.A.D. Briggs, and O.V. Kolosov, hys. Rev. B 61 (2000) 13995.

method of evaluating local elasticity and adhesion energy from the nonlinear sponse of AFM cantilever vibrations, M. Muraoka and W. Arnold, JSME Int. Series A 44 (2001) 396.